



Oldknow, K.J., Seebacher, J., Goswami, T., Villen, J., Pitsillides, A.A., O'Shaughnessy, P.J., Gygi, S.P., Schneyer, A.L., and Mukherjee, A. (2013) Follistatin-like 3 (FSTL3) mediated silencing of transforming growth factor (TGF) signaling is essential for testicular aging and regulating testis size. *Endocrinology*, 154 (3). pp. 1310-1320. ISSN 0013-7227

Copyright © 2013 The Endocrine Society

A copy can be downloaded for personal non-commercial research or study, without prior permission or charge

The content must not be changed in any way or reproduced in any format or medium without the formal permission of the copyright holder(s)

When referring to this work, full bibliographic details must be given

<http://eprints.gla.ac.uk/77647/>

Deposited on: 2 May 2013

Follistatin-like 3 (FSTL3) Mediated Silencing of Transforming Growth Factor β (TGF β) Signaling Is Essential for Testicular Aging and Regulating Testis Size

Karla J. Oldknow, Jan Seebacher, Tapasree Goswami, Judit Villen, Andrew A. Pitsillides, Peter J. O'Shaughnessy, Steven P. Gygi, Alan L. Schneyer, and Abir Mukherjee

Lifestyle Research Group, Comparative Biomedical Sciences (K.J.O., A.A.P., A.M.), Royal Veterinary College, London, United Kingdom; Department of Cell Biology (J.S., T.G., J.V., S.P.G.), Harvard Medical School, Boston, Massachusetts; Institute of Biodiversity (P.J.O.), Animal Health & Comparative Medicine, University of Glasgow, Glasgow, United Kingdom; and Department of Biology (A.L.S.), University of Massachusetts-Amherst, Amherst, Massachusetts.

Follistatin-like 3 (FSTL3) is a glycoprotein that binds and inhibits the action of TGF β ligands such as activin. The roles played by FSTL3 and activin signaling in organ development and homeostasis are not fully understood. The authors show mice deficient in FSTL3 develop markedly enlarged testes that are also delayed in their age-related regression. These FSTL3 knockout mice exhibit increased Sertoli cell numbers, allowing for increased spermatogenesis but otherwise showing normal testicular function. The data show that FSTL3 deletion leads to increased AKT signaling and SIRT1 expression in the testis. This demonstrates a cross-talk between TGF β ligand and AKT signaling and leads to a potential mechanism for increased cellular survival and antiaging. The findings identify crucial roles for FSTL3 in limiting testis organ size and promoting age-related testicular regression. (*Endocrinology* 154: 1310–1320, 2013)

Survival and maintenance of species depend on testicular development and regression timed to maximize reproduction. In most mammals, testicular size is correlated with fertility, and in humans, reduced testicular size or microorchidism is linked to infertility (1). Testicular regression is of particular importance to seasonal breeding animals (2) because this helps restrict reproduction, which demands great energy, to favorable times of the year. Testicular regression is also seen more generally with aging. Indeed, maintaining full fertility beyond the normal reproductive age risks accumulation and propagation of mutations in the germ cell genome (3, 4). Therefore, an age-related decline in testicular function and fertility is important. Despite the crucial role played in species propagation and preservation by the processes of testicular growth and regression, the cellular mechanisms that regulate them remain largely unknown.

In mammals, testis development initiates with the SRY-driven differentiation of Sertoli cells, which provide a niche for germ cell and steroidogenic cell recruitment and development (5). Sertoli cells proliferate through the second half of gestation and early neonatal life. They become mitotically quiescent shortly before puberty but are then maintained in number and continue to provide an environment for ongoing germ cell development throughout the adult reproductive life. Thus, the number of Sertoli cells in a testis is a tightly controlled key determinant of the extent of spermatogenesis (germ cell production) in the testis. Additionally, increasing Sertoli cell number and spermatogenesis beyond the normal and optimal requirement is likely to come at a metabolic cost with no added benefit to the animal.

ISSN Print 0013-7227 ISSN Online 1945-7170
Printed in U.S.A.

Copyright © 2013 by The Endocrine Society

doi: 10.1210/en.2012-1886 Received August 26, 2012. Accepted January 18, 2013.

First Published Online February 13, 2013

Abbreviations: BTB, blood-testis barrier; FBS, fetal bovine serum; FSTL3, follistatin-like 3; KO, knockout; IGF1BP, IGF binding protein; PTEN, phosphatase and tensin homolog; TBST, 50 mM Tris pH 7.5, 150 mM NaCl, 0.05% Tween 20; WT, wild-type.

Along with trophic and steroid hormones, activin and other TGF β superfamily ligands play crucial local roles during the development and maintenance of the testis and testicular function (6). The TGF β ligand signaling system comprises ligand binding-dependent activation of membrane-bound heterotetrameric receptor complexes that directly phosphorylate and activate DNA binding transcription factors. Of the TGF β factors expressed in the testis, activin is specifically inhibited by follistatin-like 3 (FSTL3), an endogenous glycoprotein also expressed in the testis (7, 8).

Here we have investigated the effects of FSTL3 deletion, and thus a misregulation of activin signaling, on testicular development and function to identify the role of this pathway in organ development, homeostasis, and longevity.

Materials and Methods

Mice

Fstl3 gene-deleted (FSTL3 KO) (9) and wild-type (WT) mice (C57BL/6) were maintained at 14:10 light-and-dark cycles. All animal studies complied with US Department of Agriculture (Protocol Number: 2005N000131/2) or UK Home Office guidelines (Project License: PPL 70/6424).

Histology and histomorphometry

Testes were isolated from mice of different ages and fixed in 4% paraformaldehyde (for immunohistochemistry) or Bouin's fixative (for histology, histomorphometry, and stereology) overnight, processed for paraffin embedding, microtome-sectioned at 6- μ m thickness, stained with hematoxylin and eosin, and imaged with a microscope. For measurement of seminiferous tubule size distribution, Adobe Photoshop size measurement tools were used on microscope images to measure the shortest diameter of seminiferous tubules of circular cross-section. Obliquely sectioned tubules were excluded from analyses.

Stereology

Stereology was performed as described previously (10). Briefly, testes were embedded in Technovit 7100 resin, cut into 20- μ m sections, and stained with Harris' hematoxylin. The optical dissector technique (11) was used to count the number of Leydig, Sertoli, and germ cells in each testis. Sertoli and germ cells were identified by their distinctive nuclei and position within the tubule, whereas the Leydig cells were identified by their position within the interstitial tissue and their round nuclei and prominent nucleoli, as described previously (10). The numerical density of each cell type was estimated using an Olympus BX50 microscope fitted with a motorized stage (Prior Scientific Instruments, Cambridge, United Kingdom) and Stereologer software (Systems Planning Analysis, Alexandria, Virginia).

Immunofluorescence and immunohistochemistry

Immunolocalization was performed as described previously (9). Briefly, paraffin-embedded tissue sections were dewaxed in

xylenes and rehydrated, and antigen was retrieved with 0.01 M sodium citrate buffer. The sections were incubated in PBS containing 0.1% Triton X-100 for 20 minutes and washed and incubated in 10% horse serum in PBS for 1 hour at room temperature. Sections were incubated with primary antibodies at recommended dilutions at 4°C overnight. The primary antibodies used were rabbit polyclonal antibodies against phospho-SMAD2 (pSMAD2; Millipore, Billerica, Massachusetts), AKT and SIRT1 (Cell Signaling Technology, Beverly, Massachusetts). For double immunofluorescence using pSMAD2 (Millipore) and SIRT1 (Cell Signaling Technology) rabbit polyclonal antibodies, the staining was performed sequentially as described before (12). First, SIRT1 antibody was probed with Alexa Fluor 594 conjugated goat antirabbit IgG (Invitrogen, Grand Island, New York) followed by extensive washes and then incubation with pSMAD2 antibody, probed with Alexa Fluor 488 conjugated goat antirabbit IgG (Invitrogen). Sections were mounted using fluorescent mounting medium (Vector Labs, Burlingame, California) and photographed using a Leica DM4000B fluorescence microscope (Leica Microsystems, Wetzlar, Germany). Appropriate controls to address specificity of secondary antibodies and experiments with single antibodies were also performed to ensure double immunolocalization was not an artifact. For immunohistochemical detection, the sections were processed with an antirabbit Vectastain Elite ABC kit (Vector Labs) and NovaRed substrate kit (Vector Labs).

Microdensitometry

Serial 6- μ m sections of WT and FSTL3 KO mouse testes were immunohistochemically labeled for detection of phospho-SMAD2, as described above. Labeling intensity was measured in cells located at the periphery (early, E) and intermediate and central (late, L) zones of seminiferous tubules using a Vickers M85A scanning and integrating microdensitometer at 550 nm (Vickers Limited, York, United Kingdom) (13). At least eight cells in each zone, in multiple tubules, in each of five sections from WT and FSTL3 KO mouse testes were evaluated.

Flow cytometry

Flow cytometric analyses of testicular cells were performed as described previously (14). Briefly, testes were dissected, decapsulated, and incubated in 0.25-mg/mL collagenase type 3 (Sigma, St Louis, Missouri) at 32°C for as long as 30 minutes with agitation. Dispersed tubules were washed twice in PBS and incubated with 0.25 mg/mL trypsin (Gibco-BRL, Grand Island, New York) and 1 mg/mL DNaseI (Sigma) at 32°C for 10 minutes with agitation. Trypsin digestion was terminated by adding an equal volume of DMEM containing 10% fetal bovine serum (DMEM/FBS). Digested tubules were collected by centrifugation and resuspended by gentle trituration in DMEM/FBS to obtain a single-cell suspension. This was filtered through a 50- μ m mesh (Costar Inc, Corning, New York), stained with trypan blue and counted in a hemocytometer. Germ cell suspensions were stained with propidium iodide (PI) for DNA content and nuclear size analysis. Then 2×10^5 cells were rinsed once with balanced salt solution, resuspended in 0.2 mL cold PI staining solution (10 mM Tris, pH 8.0, 150 mM NaCl, 0.1% Nonidet P40, 10 μ g/mL RNaseA, and 50 μ g/mL PI), vortexed for 2 to 3 seconds and incubated on ice for 10 minutes to lyse the plasma membrane and stain nuclear DNA. Nuclear size and complexity and DNA content were de-

terminated on a BD Canto II analyzer (Becton Dickinson, Franklin Lakes, New Jersey) with PI detected in the phycoerythrin channel with linear amplification. The forward scatter and side scatter profiles were gated as described before (14) to identify germ cell populations.

RNA expression data mining

Gene expression omnibus data sets were searched for gene expression during mouse spermatogenesis, and the spermatogenesis and testis development time course (MG-U74B) data set was selected as the primary data source. Data between two time points during testis development were compared, and significantly altered mRNA were identified using a two-tailed *t* test with a significance level of $P < .05$. Genes expressed differentially during the time windows of 0 to 14, 20 to 35 and 20 to 56 days (corresponding to somatic expansion, first wave of spermatogenesis, and spermatogenesis to postpubertal development, respectively) in comparison with the rest of the time windows were thus identified.

Quantitative proteomics

Briefly, WT and KO testes were lysed and the lysates sonicated in urea containing lysis buffer. Equal amounts of these lysates were reduced and alkylated, then digested with trypsin. Tryptic digests were desalted, and peptides were labeled with normal (no isotope label) for WT or heavy (d6) for FSTL3 KO dimethyl groups (15). WT and KO peptides were then mixed and separated by reverse phase liquid chromatography and detected in a hybrid dual-cell quadrupole linear ion trap-orbitrap mass spectrometer (LTQ Orbitrap Velos, Thermo Fisher Scientific Products, Waltham, Massachusetts) using a data-dependent Top 20 method. After acquisition of mass spectrometry data, image file format RAW files were processed with software developed in-house. Tandem mass spectrometry (MS/MS) spectra were searched against a composite database containing the mouse International Protein Index database and reversed “decoy” versions of these proteins using the SEQUEST algorithm. Peptide quantification was performed using the VISTA algorithm. Additional details are provided in the Supplemental Materials published on The Endocrine Society’s Journals Online web site at <http://endo.endojournals.org>.

Testis Explant Cultures

Wild-type mice were euthanized using CO₂, and testes were dissected using aseptic techniques. Dissected testes were detunicated, rapidly divided into six parts using sharp tweezers, washed in OptiMEM (Gibco-BRL, Grand Island, New York) containing antibiotics, and gently teased to loosen tubules. These were then cultured in OptiMEM in the presence or absence of either 25 ng/mL activin (PeproTech, Rocky Hill, New Jersey) or 100 ng/mL FSTL3 (R&D Systems, Minneapolis, Minnesota) for 16 hours at 32°C. At the end of treatment, protein lysates were prepared from these cultured testis explants.

Preparation of tissue lysates and Western blotting

Frozen tissue samples were pulverized in dry ice and homogenized in lysis buffer (50 mM Tris-HCl, pH 7.4, 1% NP-40, 150 mM NaCl, 20 mM NaF, 10 mM Na₂P₂O₇, 1 mM Na₃VO₄) supplemented with a mixture of protease inhibitors (Complete Mini, Roche Applied Science, Indianapolis, Indiana). Fresh tis-

sue was directly placed in lysis buffer and homogenized. This homogenate was then sonicated at low power to shear chromosomal DNA and centrifuged to remove debris. Protein concentrations were estimated using a Bradford colorimetric assay (Bio-Rad Laboratories, Hercules, California). Fifty micrograms total protein lysate was loaded on 10% sodium dodecyl sulfate polyacrylamide gel electrophoresis gels and size-separated using constant current. After electrophoresis, proteins were transferred from gels to pure nitrocellulose membranes (Little Chalfont, Buckinghamshire, United Kingdom) and efficiency of transfer assessed by Ponceau-S staining. The membranes were then washed in TBST (50 mM Tris pH 7.5, 150 mM NaCl, 0.05% Tween 20) and incubated with blocking buffer (5% nonfat dry milk in TBST) at room temperature for 1 hour. Protein blots were incubated with primary antibodies (used at recommended dilutions in blocking buffer) overnight at 4°C. Membranes were washed three times with TBST and incubated with appropriate horseradish peroxidase conjugated secondary antibodies (Sigma). The membranes were again washed four times, and immune complexes formed on the blot were visualized by enhanced chemiluminescence (ECL; Amersham Biosciences). Immunoreactive protein bands were analyzed using the public domain National Institutes of Health Image program (developed at the United States National Institutes of Health and available on the Internet at <http://rsb.info.nih.gov/nih-image/>). Of the AKT antibodies used in this study, pan-AKT antibody reacts to all three forms of AKT, and phosphoAKT antibody identifies AKT phosphorylated at Ser473.

Statistical analysis

Student paired two-tailed *t* test was performed using statistical analysis functions in Prism 3.0 (GraphPad, La Jolla, California) or Excel (Microsoft, Redmond, Washington). Differences between the comparison groups were considered statistically significant at $P < .05$.

Results

FSTL3 deletion increases testicular size and delays testicular regression

To identify the effects of FSTL3 deletion on the testis, we first compared testes from WT and *Fstl3* gene-deleted (FSTL3 KO) (9) mice, and as shown in Figure 1, A and B, FSTL3 deletion causes marked testicular enlargement. The increase in testicular size is not associated with any corresponding significant increase in epididymal sperm count (Figure 1C) or serum testosterone levels (Figure 1D). These findings suggest that the mechanisms involved in sperm output and endocrine regulation of steroidogenesis are intact in FSTL3 KO mice. Importantly, reproductive parameters (interlitter interval, litter size) are not altered in FSTL3 KO mice (Figure 1, E and F). In addition, histologic examination shows that testis structure in FSTL3 KO is grossly similar to that in WT, with no visible pathologies (Figure 2A, top row). Therefore, FSTL3 deletion selectively increases the size of testes without affecting gross testicular structure or function.

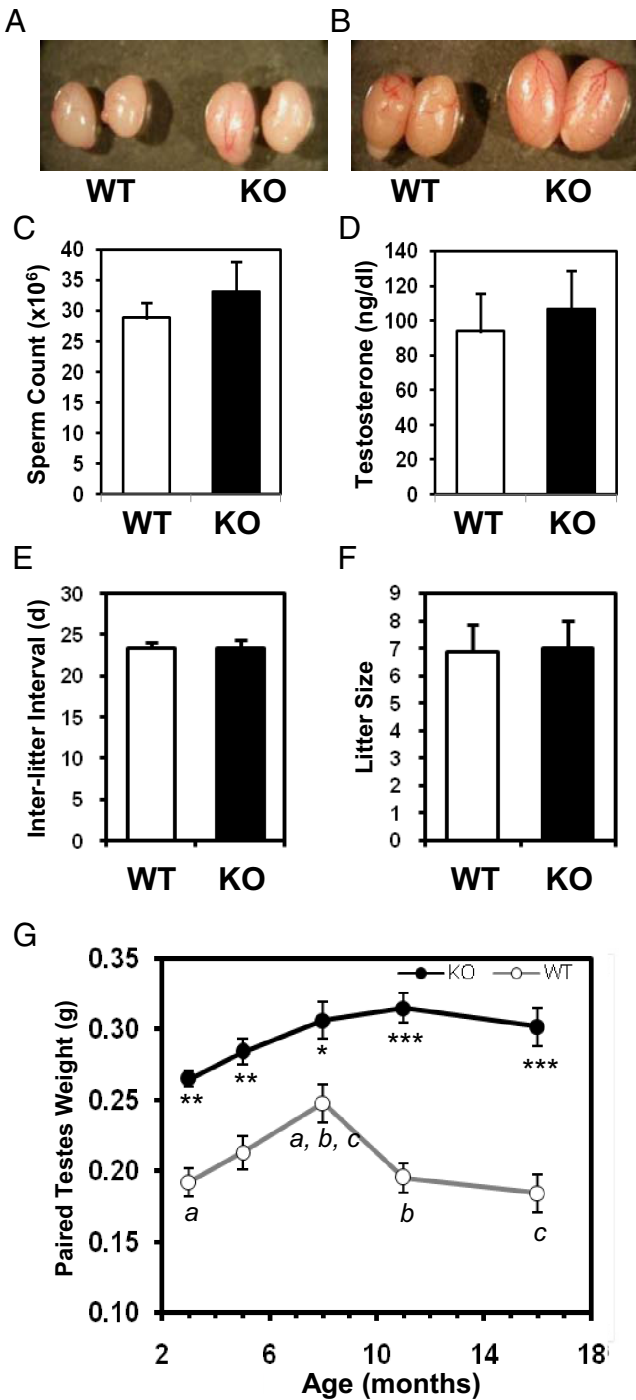


Figure 1. Follistatin-like 3 (FSTL3) is important in limiting testicular size and inducing testicular regression in mice. Photographs showing enlarged testes in *Fstl3*^{-/-} (FSTL3 knockout [KO]) compared to wild-type (WT) mice at 3 mo (A) and 10 mo (B), respectively. Bar graphs showing epididymal sperm counts from 6-mo-old WT (n = 10) and FSTL3 KO (n = 10) mice (C); serum testosterone levels from age-matched WT (n = 10) and KO (n = 22) animals (D); interlitter interval in days (d) (E) and litter size (F) in WT and KO mating pairs (n = 4 pairs, 3–4 litters). Graph of paired testes weights plotted against mean age of WT and FSTL3 KO mice (G). Testes were significantly larger in KO mice than WT mice at all ages measured. Although WT mice show a decrease in testicular weight with age, such regression is not seen in the FSTL3 KO mice. Error bars = SEM; a, b, *P < .05; c, **P < .01; ***P < 10⁻⁵.

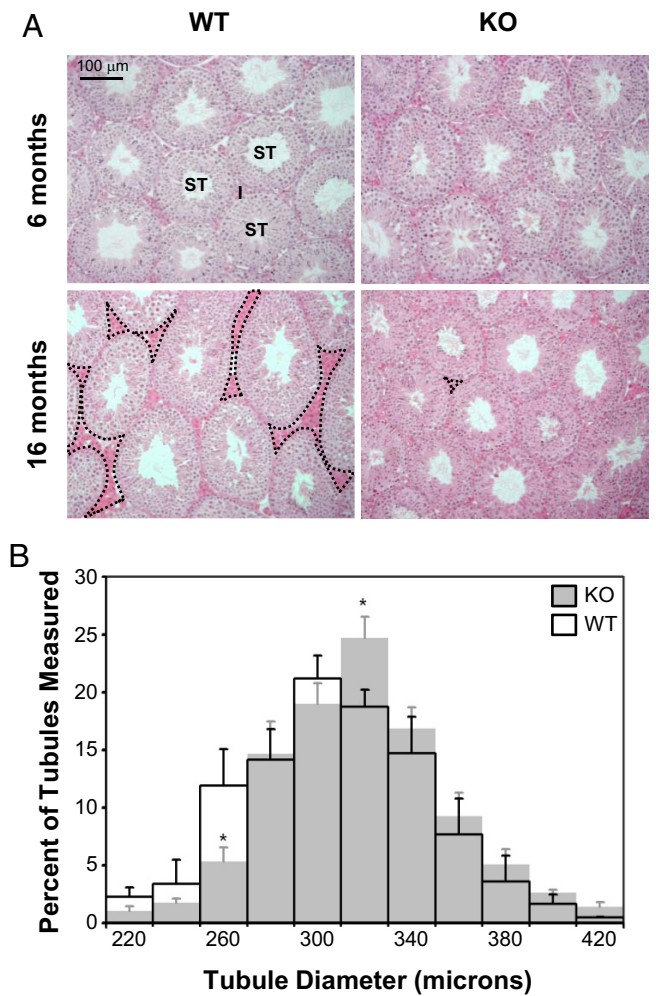


Figure 2. Follistatin-like 3 (FSTL3) deletion leads to the maintenance of testicular size with age. Hematoxylin and eosin staining of testes sections from wild-type (WT, left) and FSTL3 knockout (KO, right) animals at 6 mo (top) and 16 mo (bottom), shown at 20× magnification (I, interstitial/Leydig cells; ST, seminiferous tubule). There appears to be more interstitial space in the testes of WT (some with dotted outline) than in FSTL3 KO animals at 16 mo. Scale bar represents 100 μm (A). Seminiferous tubule size distribution in FSTL3 KO and WT mice. The shortest diameter of seminiferous tubules of circular cross-section were measured from three hematoxylin-and-eosin-stained testicular sections (6 μm thick) at least 120 μm apart from each other for each 16-mo-old WT (transparent, n = 5 mice, 829 tubules) and FSTL3 KO (gray, n = 5 mice, 951 tubules) mouse. Error bars = SEM; *P < .05 (B).

It is possible that the increased testicular size in FSTL3 KO affects tissue homeostasis mechanisms and therefore maintenance of testis size with age. To address this, testis weight was measured at different ages and, as shown in Figure 1G, is found to increase significantly during the first 7 mo of life and subsequently decrease during the next 9 mo in WT mice. In marked contrast, no significant change in testis weight is observed in FSTL3 KO mice between 4 and 16 mo (Figure 1G). Furthermore, we found that WT testes undergoing testicular regression in aged, 16-mo-old mice show an expected reduction in the pro-

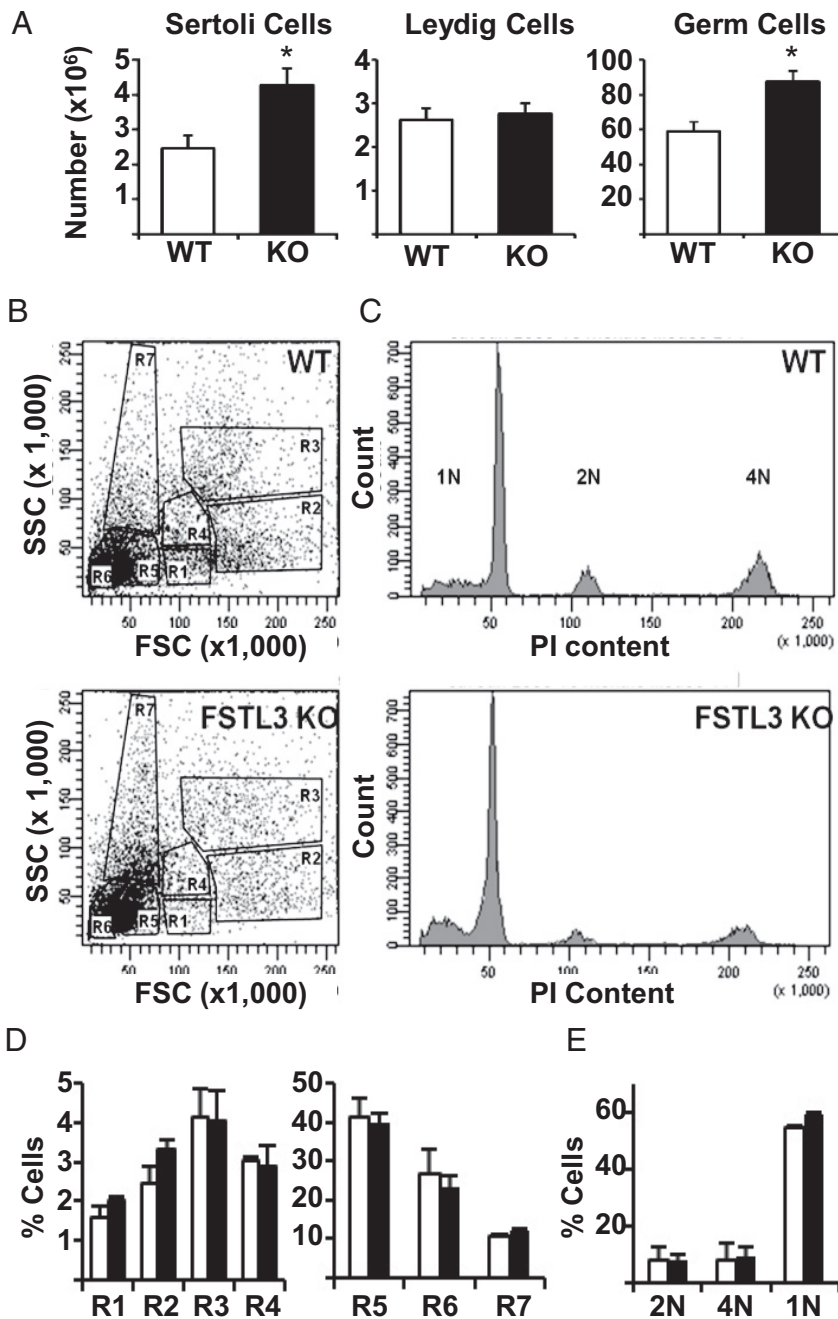


Figure 3. Sertoli cell and germ cell numbers are increased in follistatin-like 3 (FSTL3) knockout (KO) mice without affecting spermatogenic program. Stereological analysis of testes from 16-month-old WT (n = 5) and FSTL3 KO (n = 5) mice presented as bar graphs showing increased Sertoli and germ cells, whereas Leydig cell numbers are unaltered (A). Profiling germ cell development in 16-month-old FSTL3 KO mice by flow cytometry (B–E). Flow cytometric profiles of germ cell suspensions prepared from WT (top) and FSTL3 KO (bottom) testes (B). DNA content profiles of testicular cells from WT (top) or FSTL3 KO (bottom) (C). Percentages of total number of cells present in each of the populations from B and C (n = 3) are presented as column graphs in D and E, respectively. R1, premeiotic 2N spermatogonia; R2, 4N primary spermatocytes; R3, late-stage spermatocytes; R4, postmeiotic secondary spermatocytes; R5, round spermatid; R6, elongated spermatid; R7, spermatozoa. Error bars = SEM, *P < .05.

2A, right column). These novel findings suggest that FSTL3 acts to restrict both the proliferation and longevity of testicular cells.

FSTL3 deletion increases Sertoli and germ cell numbers

Spermatogenesis in mice occurs as a wave along the length of the seminiferous tubule, so tubule thickness corresponds to the stages of spermatogenesis: constricted at initial stages and dilated at the final stages of spermatogenesis (16). Testicular size is, in turn, dependent upon the total length of the seminiferous tubules. Because testicular architecture appears largely unaffected in FSTL3 KO mice, it is likely that the increased testicular size is attributable to greater total seminiferous tubule length and therefore more Sertoli cells and associated germ cells, the main components of the seminiferous tubules. Measurements of seminiferous tubule width distribution in 16-month-old mice (Figure 2B) revealed a greater number of tubules with increased width in FSTL3 KO mice, suggesting the possibility of increased spermatogenesis in the absence of FSTL3. Indeed, stereological analyses (10) show increased Sertoli and germ cell numbers in FSTL3 KO compared with WT mice, but there is no difference in Leydig cell numbers (Figure 3A).

To investigate whether the spermatogenic program is altered in FSTL3 KO testes, flow cytometry of whole testicular dispersates was performed. An analysis of the distribution of the different spermatogenic cell stages (14) reveals that there is no stage-selective modification in these populations of cells in FSTL3 KO testes (Figure 3, B and D) compared with WT testes. Moreover, when sorted for DNA content, there also is no difference between WT and FSTL3 KO mice in the proportions of cells containing 4N (mitotically dividing diploid), 2N (diploid) and 1N (haploid

portion of the seminiferous tubule compartment (Figure 2A, left column). In contrast, structural integrity of the testis is maintained at 16 mo in FSTL3 KO mice (Figure

FSTL3 KO mice in the proportions of cells containing 4N (mitotically dividing diploid), 2N (diploid) and 1N (haploid

and sperm) equivalent DNA (Figure 3, C and E). These analyses indicate that FSTL3 KO mice have increased Sertoli cell numbers and suggest that this leads to a net increase in germ cell numbers without affecting the spermatogenic program.

Signaling pathways are altered in the testes of FSTL3 KO mice

Increased Sertoli cell number is therefore the underlying cause of increased testis size in FSTL3 KO mice. Genetic mouse models of FSH, testosterone, activin, and IGF1 action show that these factors affect Sertoli cell numbers (17–20). However, increased exposure to FSH, androgen, or activin does not increase Sertoli cell number (21–23). To identify pathways that might underpin the increased Sertoli cell numbers in FSTL3 KO mice, we mined previously reported microarray RNA expression data and compared gene expression patterns between early (0–14 d) and late (20–35 and 20–56 d) stages of testes maturation (Supplemental Figure 1). This revealed that *Igfbp3* and *Igfbp5*, encoding IGF binding proteins 3 (IGFBP3) and 5 (IGFBP5), respectively, are

among genes that are expressed highly during early postnatal testicular development, a period when Sertoli cell expansion occurs, but have reduced expression at later stages. Because these proteins are critical negative regulators of IGF1 signaling, it is likely that the growth stimulatory effects of IGF1 are closely regulated during Sertoli cell expansion. Furthermore, IGF1 receptors are expressed in multiple cell types within the testis, including Sertoli cells (19), making it likely that Sertoli cells will be prone to IGF1-dependent effects. Thus, a mechanism of restricting Sertoli cell proliferation within testes might include the curtailment of IGF1 signaling. It is possible, therefore, that increased Sertoli cell numbers in FSTL3 KO testes might arise from increased IGF1 signaling.

Consistent with a role for increased IGF1 action in the expansion of Sertoli cell numbers, we found that AKT, a known downstream effector of IGF1 signaling, exhibits increased levels of activation in FSTL3 KO testes (Figure 4A), as estimated by calculating the ratio of AKT phosphorylated at Ser473 to total AKT, assayed by a panAKT

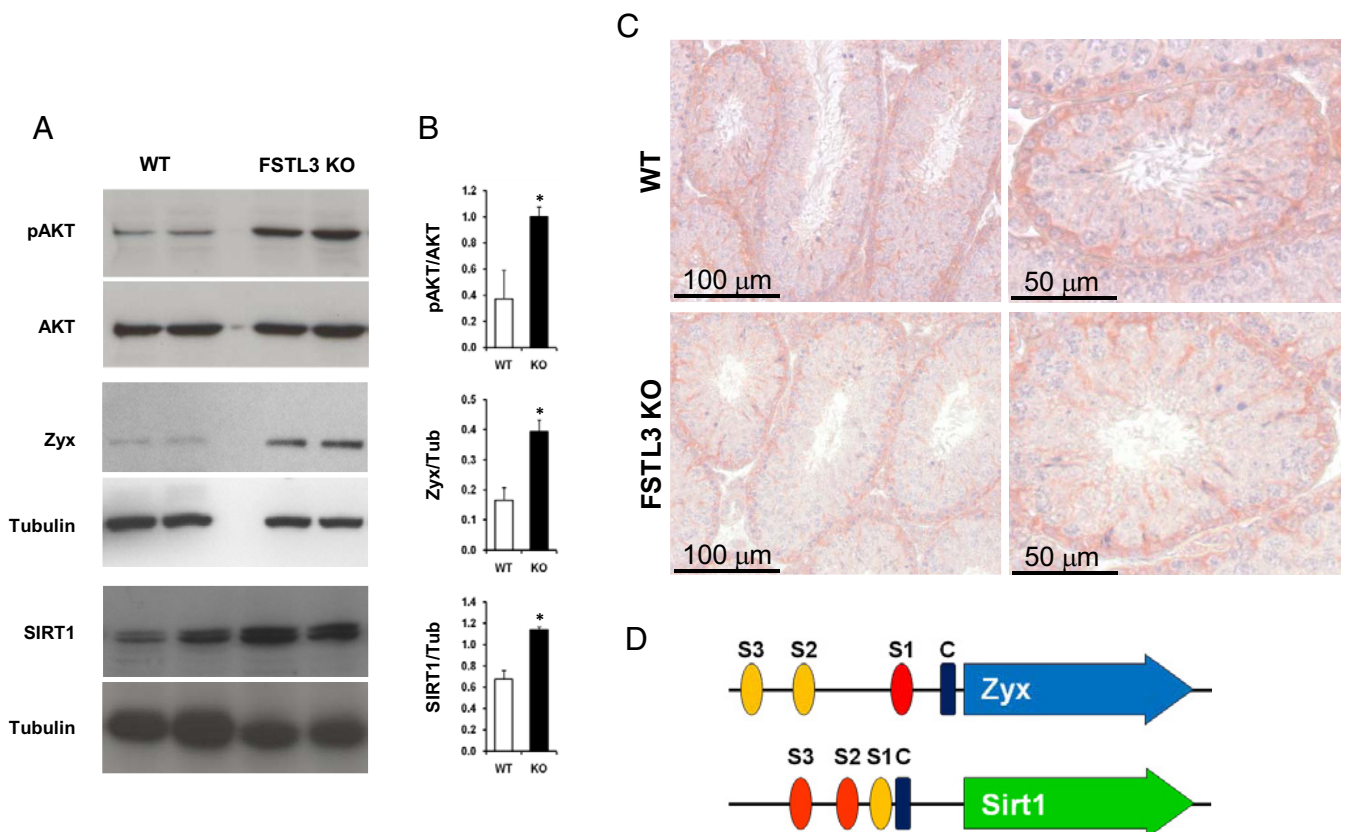


Figure 4. Follistatin-like 3 (FSTL3) deletion causes induction of proliferative and antiaging pathways. A series of Western blot analyses of lysates from wild-type (WT) and FSTL3 knockout (KO) testes showing phospho-AKT (pAKT), AKT (relative molecular mass, MAR: 60 kDa), SIRT1 (Mr: 120 kDa), zyxin (Mr: 65 kDa) and tubulin (Mr: 65 kDa, internal control), as indicated (A). Adjacent bar graphs presented (B) show the respective ratio of expression in WT and FSTL3 KO, as indicated, obtained from densitometric analyses of these Western blots. Immunohistochemistry showing localization of AKT in Sertoli and germ cells in WT (top) and FSTL3 KO (bottom) testis sections. Scale bar represents 100 and 50 μm , as indicated (C). Schematic representation of *Zyx* and *Sirt1* gene promoters showing the location of putative SMAD binding sites (S1, S2, S3) and CCAAT enhancer box (designated "C") (D). SMAD binding elements are depicted as red ovals, whereas partial SMAD binding elements are orange. The CAAT is represented by a blue rectangle. The gene transcripts are shown as colored arrows. Error bars = SEM; * $P < .05$.

antibody that identifies all AKT isoforms. A key promoter of the cell cycle is β -catenin which is targeted for proteasomal degradation upon phosphorylation by GSK3 β . AKT activation can maintain continued cell-division by phosphorylating and thus down-regulating GSK3 β activity to block β -catenin degradation. Immunoblotting shows that GSK3 β phosphorylation is increased, along with a concomitant increase in β -catenin levels, in FSTL3 KO compared with WT testes (Supplemental Figure 2). Immunohistochemistry reveals that the level of AKT expression, in terms of levels and localization, is similar in the WT and FSTL3 KO testes and is restricted to Sertoli and germ cells (Figure 4C). Thus, it appears that alteration of AKT activation is the crucial difference between WT and FSTL3 KO testes. Together these findings strongly suggest a putative role for IGF1-dependent increases in AKT activation in promoting Sertoli cell proliferation and spermatogenesis in the enlarged testes of FSTL3 KO mice.

A possible mechanism for testicular regression is increased apoptosis of spermatogenic cells. To examine whether the observed lack of testicular regression in FSTL3 KO mice involves reduced levels of apoptosis, we monitored the extent of apoptosis by terminal deoxynucleotidyl transferase dUTP nick end labeling (TUNEL) assays on testicular sections and found reduced apoptosis in FSTL3 KO compared with WT (Supplemental Figure 3). To identify proteins that might be involved in blocking age-related testicular regression in FSTL3 KO mice, we used quantitative mass-spectrometry-based proteomics (15). We identified 12 and 8 proteins that are significantly

up-regulated and down-regulated, respectively, in FSTL3 KO mice testes compared with those of WT mice at 16 mo (Figure 5, Supplemental Table 1). It is likely that some of these candidate proteins are: involved in the maintenance of testis size and function or active in down-regulating testis size with age. Zyxin, which is known to play a key role in spermatogenesis by facilitating Sertoli-to-germ cell connections (24), is among the proteins up-regulated in FSTL3 KO testes. Zyxin is known to interact with Sirtuin-1 (SIRT1) (25), a protein promoting antiaging pathways (26), which is necessary for spermatogenesis (27). In addition, nuclear accumulation of zyxin and SIRT1 has been shown to promote cell survival, and AKT-mediated zyxin phosphorylation can repress apoptosis (28, 29). Thus, we examined the expression of zyxin and SIRT1 in FSTL3 KO mouse testes. Confirming mass-spectrometry data, immunoblotting shows increased expression of zyxin and SIRT1 proteins in FSTL3 KO testes compared with those of WT (Figure 4A). These data are consistent with a role for zyxin and SIRT1 in blocking apoptosis and promoting cell survival, which likely contributes to the lack of age-related regression of the FSTL3 KO testis.

Examination of the *zyxin* (*Zyx*) and *Sirt1* gene promoter regions identified canonical SMAD binding sites (Figure 4D), supporting the possibility that these genes are induced by activin. Increased activin signaling, reflected by our finding of increased SMAD2 activation in FSTL3 KO testes (Supplemental Figure 4), might therefore result in increased expression of zyxin and SIRT1. Importantly, the extent of SMAD 1/5 phosphorylation was not altered

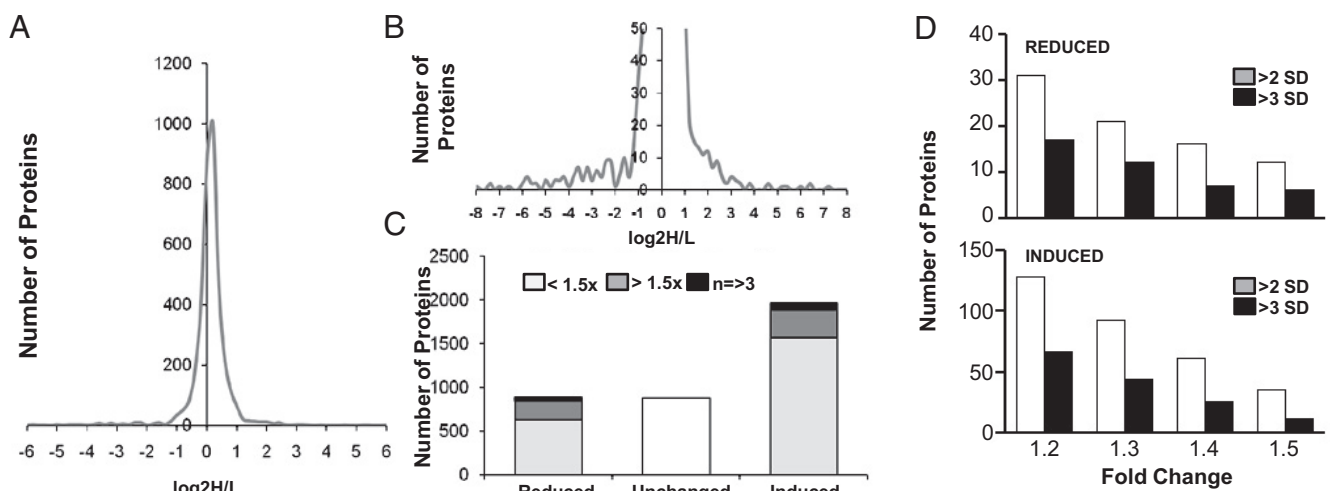


Figure 5. Quantitative mass spectrometry reveals changes in the follistatin-like 3 (FSTL3) knockout (KO) testis proteome. An overview of quantitative mass spectrometry results presented as a distribution curve of number of proteins versus the ratio of comparative protein expression between KO and wild-type (WT) (A). An enlargement of the curve in A showing the distribution of comparative expression of proteins from which candidate proteins were identified (B). Bar graph showing the number of proteins that are reduced, unchanged, and increased in KO compared with WT (C). Number of proteins reduced (top) or induced (bottom) in the testis of 16-mo-old FSTL3 KO mice by 1.2- to 1.5-fold over those of WT mice, as indicated. Number of proteins with mean fold expression > 2 SD and > 3 SD are shown (D).

in FSTL3 KO testes (Supplemental Figure 4). Indeed, our immunofluorescent labeling reveals that SIRT1 is expressed in the same cells as phosphorylated SMAD2 in the testes (Figure 6A). In addition, although exogenous activin does not induce SIRT1 expression in WT testis explants, possibly because endogenous Sertoli cell-derived activin might produce maximal activation of the *Sirt1* promoter, exogenous FSTL3 down-regulates SIRT1 expression, most likely by blocking the activity of endogenous activin (Figure 6, B and C). These data support the hypothesis that FSTL3 reduces activin-dependent SIRT1 expression in normal spermatogenic cells.

Discussion

Endogenous ligand inhibitors provide a means of modulating or restricting TGF β ligand signaling. Among these inhibitors, the glycoprotein FSTL3 binds and inhibits activin, myostatin, and GDF11. In the current study, we demonstrate that deletion of FSTL3 and thus removal of FSTL3-dependent inhibition of activin action has profound effects on the development of an activin and FSTL3 sensitive organ, the testis.

Deletion of FSTL3 not only increases testicular size but also prevents age-related testicular regression. This sug-

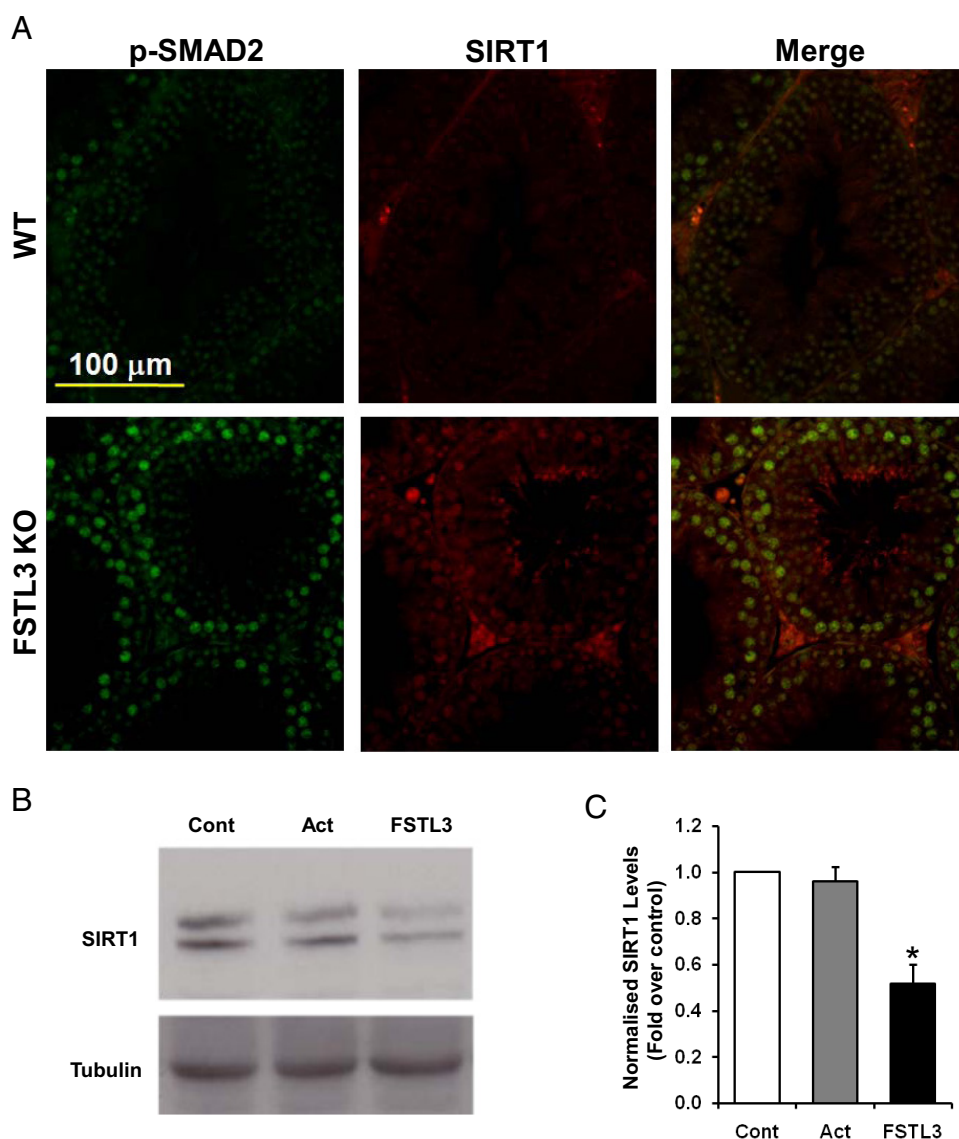


Figure 6. Follistatin-like 3 (FSTL3) and SMAD are regulators of SIRT1 expression in the testis. Dual-label immunofluorescence showing colocalization of phospho-SMAD2 (pSMAD2) and SIRT1 in the germ cells of FSTL3 knockout (KO) mouse testis sections. Scale bar represents 100 μ m (A). Western blot analyses of lysates from wild-type (WT) mice testis explants maintained in culture for 24 hours with either medium alone (Cont), recombinant activin (Act, 25 ng/mL), or FSTL3 (100 ng/mL), as indicated, showing SIRT1 and tubulin (internal control) expression (B). Adjacent bar graph (C) shows the level of SIRT1 expression, normalized to tubulin, obtained from densitometric analyses of these Western blots. Error bars = SEM; * $P < .05$.

gests that the roles played by FSTL3 and activin signaling in the testis extend from organ development to adult tissue homeostasis and are important in the determination of organ aging. We show that increased Sertoli cell numbers and an accompanying increase in germ cell numbers lead to increased testicular size in FSTL3 KO mice. However, the mere presence of Sertoli cells does not guarantee germ cell production. In support of this, transgenic overexpression of FSTL3 in the gonads results in male infertility because of the development of testes that contain seminiferous tubules with Sertoli cells but no germ cells (30). In humans this “Sertoli cell only” pathology is associated with infertility (31). In contrast, in the absence of FSTL3, we observe that both Sertoli and germ cell numbers are increased above normal levels and FSTL3 KO mice are fertile. Therefore, it is likely that a modulation of FSTL3 expression might be key to the regulation of Sertoli cell number and spermatogenesis. This finding is of crucial importance because induction of spermatogenesis in the adult is a plausible therapeutic avenue for male infertility caused by a deficiency in sperm production.

Sertoli cell expansion in testes occurs before the initiation of spermatogenesis. The number of Sertoli cells is then maintained throughout testicular life. Sertoli cells act as “nurse” cells for spermatogenesis; therefore, the extent of spermatogenesis is dependent on the number of Sertoli cells. Thus, the maximal testicular size is dependent on the number of Sertoli cells present within the testis. The increased number of Sertoli cells in FSTL3 KO mice is congruent with an increase in Sertoli cell division or a delay or reduction in an inhibitory signal that curtails Sertoli cell division. Importantly, there is a known link between establishment of the blood-testis barrier (BTB) and the onset of mitotic arrest of Sertoli cells and subsequent spermatogenesis (32). Experimental models to induce neonatal hypothyroidism that delay the onset of BTB formation (33) also prolong the Sertoli cell expansion stage, leading to increased numbers of Sertoli cells and consequently increased testicular size (34–36). However, FSTL3 expression is low in the thyroid gland and has not been linked to thyroid gland activity. In addition, there is no observed delay in puberty in FSTL3 KO mice. Thus, it is unlikely that FSTL3 deletion affects BTB formation. It is more likely that signaling pathways altered by the direct effect of the absence of FSTL3 in the FSTL3 KO testis lead to increased Sertoli cell numbers, presumably within the normal Sertoli cell expansion stage. By data mining, we identified IGFBP3 and IGFBP5 as possible candidates that might normally limit Sertoli cell numbers. These proteins are known negative regulators of IGF1, a growth factor that can induce Sertoli cell proliferation. Moreover, under conditions in which Sertoli cell numbers become limited,

for example in response to $TNF\alpha$, IGFBP3 is induced (37). We demonstrate in this study that AKT activation, an event downstream of IGF1 action, is indeed increased in FSTL3 KO testis.

Increased AKT activation in the absence of FSTL3 may be the result of one or more altered signaling events. It is known that IGFBPs are targets of ADAM12 protease-mediated degradation, and there is evidence that FSTL3 can bind to, and presumably inactivate, ADAM12 protease (38). Thus, in the absence of FSTL3, ADAM12-dependent IGFBP degradation might increase IGF1 signaling. Second, $TGF\beta$ is known to activate miRNA 216a and 217, which lead to the degradation of phosphatase and tensin homolog (PTEN) (39). Reduced PTEN can lead to increased AKT activation (39). Because in the absence of FSTL3 activin action is induced and because $TGF\beta$ and activin can signal via the same SMAD2/3-dependent transcription, it is possible that in activin target tissues in the FSTL3 KO mouse, such as the testis, PTEN is down-regulated, ultimately resulting in AKT activation. Most directly, increased activin-dependent ALK activation might, in addition to SMAD phosphorylation, lead to AKT activation. Although it will be interesting to monitor IGFBP and PTEN protein abundance during the early somatic expansion stage in FSTL3 KO testis, it has been shown that activin treatment of ovarian tumor cells can lead to AKT activation (40).

Perhaps the most crucial effect of FSTL3 deletion on testicular function is the delay in age-related testicular regression. This phenotype suggests that FSTL3-mediated regulation of activin is imperative for limiting testicular function. Importantly, an increase in testicular size does not predicate delayed testicular regression. Before our description of the testicular phenotype of FSTL3 KO mice, two other genetic mouse mutants with increased testicular size compared with WT have been described: FMR1 KO (41) and aquaporin 8 KO (42) mice. Increased testicular size in aquaporin 8 KO mice is associated with an increased germ cell:Sertoli cell ratio (42). This clearly contrasts to the phenotype in both FSTL3 KO and FMR1 KO mice, where testis enlargement is accompanied by increased Sertoli cell proliferation (43). However, unlike FSTL3 KO mice, FMR1 KO mice exhibit normal age-related testicular regression (44). This indicates that an increase in testicular size is not necessarily linked to slower age-related regression and further highlights the unique role for FSTL3 in regulating testicular size and regression.

We used a mass-spectrometry–based quantitative proteomics approach to reveal a set of candidate proteins that might be actively engaged in limiting testis function, those down-regulated in FSTL3 KO, or involved in maintaining testis function, those up-regulated in FSTL3 KO. It is likely

that some of these proteins, particularly those up-regulated in FSTL3 KO testis, are directly regulated by increased activin signaling. Although it will be important to identify the roles of these candidate proteins in regulating tissue homeostasis, specifically in the testis as well as more generally, we focused our studies on the protein zyxin. Zyxin is a multifunctional adaptor protein enriched in the Sertoli and germ cells of the testis (24). It is a component of the actin-based adherens junction and microtubule-based desmosome-like junctions between Sertoli and germ cells (24). Importantly, zyxin is a target of AKT, and phosphorylated zyxin can bind and inhibit the proapoptotic function of acinus. In addition, zyxin function is dependent on its interaction with SIRT1, a member of the mammalian sirtuin family of proteins that promote antiaging mechanisms (26). Crucially, we found zyxin and SIRT1 expression and AKT phosphorylation significantly induced in the testis of aged FSTL3 KO mice in comparison with WT mice of the same age. AKT-dependent phosphorylation and thus inactivation of GSK3 β and levels of β -catenin, normally targeted for degradation by GSK3 β , were also induced in FSTL3 KO mice. AKT-mediated maintenance of β -catenin promotes cell survival. Therefore, with activated AKT as a major signaling hub, subsequent pathways to promote cellular survival and reduce apoptosis are activated in FSTL3 KO testes.

The main signaling pathway altered in the absence of FSTL3 is, of course, increased activin action, the primary effect of which is prolonged or increased SMAD2 activation. Thus, a direct route of gene regulation will involve binding of phosphorylated SMADs 2 and 3, complexed with SMAD4, to SMAD binding elements on target genes. Very little is known about *Sirt1* and *Zyx* gene regulation, although recent reports suggest roles for p53, CREB, and ChREB in the regulation of *Sirt1* gene (45, 46). The presence of canonical SMAD binding elements in the proximal promoter region of both *Zyx* and *Sirt1* genes suggests that their expression might be induced upon SMAD binding. Our experimental data support this possibility; activated SMAD2 and SIRT1 are coexpressed within the same cells of the testes, and FSTL3 treatment down-regulates SIRT1 expression in testicular cells in vitro.

The current study demonstrates that the deletion of FSTL3 leads to increased Sertoli cell and associated germ cell numbers, increased testicular size, and lengthened testicular life. We propose a molecular mechanistic model (Supplemental Figure 5) in which increased activin, AKT, and SIRT1 action delay the age-related curtailment of testicular function and lead to prolonged spermatogenesis during aging in these mice. Activin normally promotes testicular function, and FSTL3 regulates the extent of activin action. In the absence of FSTL3, activin action is

increased and AKT-dependent signaling is induced, either directly in response to activin binding to its receptors and a receptor-mediated signaling event or indirectly via a loss of FSTL3-mediated inhibitory actions. Therefore, AKT action-dependent cell survival mechanisms are induced: AKT-mediated phosphorylation and thus inhibition of GSK3 β increases β -catenin, a promoter of cell growth, and AKT-mediated zyxin phosphorylation activates zyxin protein, inhibiting acinus, a promoter of cell apoptosis. An interaction partner for zyxin function is SIRT1. Both zyxin and SIRT1 are induced in the testis in FSTL3 KO in an activin-induced SMAD-dependent manner. SIRT1 action contributes to antiaging effects, thus prolonging testicular function in the FSTL3 KO mouse. This model may provide a novel mechanistic basis for the regulation of testicular size and male reproductive longevity. It indicates multiple roles for FSTL3 in normal testicular function, likely to involve essential negative modulation of cellular proliferation, and in the promotion of normal testicular aging.

Acknowledgments

We thank Professor Martin Sheldon for help with mouse work and Shanta Cariese for help with flow cytometry.

Address all correspondence and requests for reprints to: Abir Mukherjee, Ph.D., Department of Comparative Biomedical Sciences, Royal Veterinary College, Royal College Street, London, NW1 0 TU, United Kingdom. E-mail: amukherjee@rvc.ac.uk.

This work was supported by Start-up and Internal Grant Scheme funding provided by the Royal Veterinary College (RVC), London, and Biotechnology and Biological Sciences Research Council equipment grant BB/F011180/1 (to A.M.), RVC Student Project Grant (to K.J.O.), BBSRC and Arthritis Research United Kingdom support (to A.P.) and by National Institutes of Health Grant R01HD39777/DK076143 (to A.L.S.).

Disclosure Summary: The authors have nothing to disclose.

References

1. Steeno OP. Clinical and physical evaluation of the infertile male: testicular measurement or orchidometry. *Andrologia*. 1989;21:103–112.
2. Turek FW, Campbell CS. Photoperiodic regulation of neuroendocrine-gonadal activity. *Biol Reprod*. 1979;20:32–50.
3. Salisbury GW, Hart RG. Gamete aging and its consequences. *Biol Reprod Suppl*. 1970;2:1–13.
4. Hardwick RJ, Tretyakov MV, Dubrova YE. Age-related accumulation of mutations supports a replication-dependent mechanism of spontaneous mutation at tandem repeat DNA loci in mice. *Mol Biol Evol*. 2009;26:2647–2654.
5. Wilhelm D, Palmer S, Koopman P. Sex determination and gonadal development in mammals. *Physiol Rev*. 2007;87:1–28.
6. Itman C, Mendis S, Barakat B, Loveland KL. All in the family:

- TGF-beta family action in testis development. *Reproduction*. 2006;132:233–246.
7. Sidis Y, Mukherjee A, Keutmann H, Delbaere A, Sadatsuki M, Schneyer A. Biological activity of follistatin isoforms and follistatin-like-3 is dependent on differential cell surface binding and specificity for activin, myostatin, and bone morphogenetic proteins. *Endocrinology*. 2006;147:3586–3597.
 8. Tsuchida K, Arai KY, Kuramoto Y, Yamakawa N, Hasegawa Y, Sugino H. Identification and characterization of a novel follistatin-like protein as a binding protein for the TGF-beta family. *J Biol Chem*. 2000;275:40788–40796.
 9. Mukherjee A, Sidis Y, Mahan A, et al. FSTL3 deletion reveals roles for TGF-beta family ligands in glucose and fat homeostasis in adults. *Proc Natl Acad Sci U S A*. 2007;104:1348–1353.
 10. Baker PJ, O'Shaughnessy PJ. Role of gonadotrophins in regulating numbers of Leydig and Sertoli cells during fetal and postnatal development in mice. *Reproduction*. 2001;122:227–234.
 11. Wreford NG. Theory and practice of stereological techniques applied to the estimation of cell number and nuclear volume in the testis. *Microsc Res Tech*. 1995;32:423–436.
 12. Gill R, Hitchins L, Fletcher F, Dhoot GK. Sulf1A and HGF regulate satellite-cell growth. *J Cell Sci*. 2010;123:1873–1883.
 13. Bastow ER, Lamb KJ, Lewthwaite JC, et al. Selective activation of the MEK-ERK pathway is regulated by mechanical stimuli in forming joints and promotes pericellular matrix formation. *J Biol Chem*. 2005;280:11749–11758.
 14. Coultas L, Bouillet P, Loveland KL, et al. Concomitant loss of proapoptotic BH3-only Bcl-2 antagonists Bik and Bim arrests spermatogenesis. *EMBO J*. 2005;24:3963–3973.
 15. Tolonen AC, Haas W, Chilaka AC, Aach J, Gygi SP, Church GM. Proteome-wide systems analysis of a cellulosic biofuel-producing microbe. *Mol Syst Biol*. 2011;7:461.
 16. Parvinen M. Regulation of the seminiferous epithelium. *Endocr Rev*. 1982;3:404–417.
 17. Dierich A, Sairam MR, Monaco L, et al. Impairing follicle-stimulating hormone (FSH) signaling in vivo: targeted disruption of the FSH receptor leads to aberrant gametogenesis and hormonal imbalance. *Proc Natl Acad Sci USA*. 1998;95:13612–13617.
 18. Archambeault DR, Yao HH. Activin A, a product of fetal Leydig cells, is a unique paracrine regulator of Sertoli cell proliferation and fetal testis cord expansion. *Proc Natl Acad Sci USA*. 2010;107:10526–10531.
 19. Nef S, Verma-Kurvari S, Merenmies J, et al. Testis determination requires insulin receptor family function in mice. *Nature*. 2003;426:291–295.
 20. Johnston H, Baker PJ, Abel M, et al. Regulation of Sertoli cell number and activity by follicle-stimulating hormone and androgen during postnatal development in the mouse. *Endocrinology*. 2004;145:318–329.
 21. Kumar TR, Palapattu G, Wang P, et al. Transgenic models to study gonadotropin function: the role of follicle-stimulating hormone in gonadal growth and tumorigenesis. *Mol Endocrinol*. 1999;13:851–865.
 22. Tanimoto Y, Tanimoto K, Sugiyama F, et al. Male sterility in transgenic mice expressing activin betaA subunit gene in testis. *Biochem Biophys Res Commun*. 1999;259:699–705.
 23. Matzuk MM, DeMayo FJ, Hadsell LA, Kumar TR. Overexpression of human chorionic gonadotropin causes multiple reproductive defects in transgenic mice. *Biol Reprod*. 2003;69:338–346.
 24. Lee NP, Mruk DD, Conway AM, Cheng CY. Zyxin, axin, and Wiskott-Aldrich syndrome protein are adaptors that link the cadherin/catenin protein complex to the cytoskeleton at adherens junctions in the seminiferous epithelium of the rat testis. *J Androl*. 2004;25:200–215.
 25. Fujita Y, Yamaguchi A, Hata K, Endo M, Yamaguchi N, Yamashita T. Zyxin is a novel interacting partner for SIRT1. *BMC Cell Biol*. 2009;10:6.
 26. Cohen HY, Miller C, Bitterman KJ, et al. Calorie restriction promotes mammalian cell survival by inducing the SIRT1 deacetylase. *Science*. 2004;305:390–392.
 27. Coussens M, Maresh JG, Yanagimachi R, Maeda G, Allsopp R. SIRT1 deficiency attenuates spermatogenesis and germ cell function. *PLoS One*. 2008;3:e1571.
 28. Kato T, Muraski J, Chen Y, et al. Atrial natriuretic peptide promotes cardiomyocyte survival by cGMP-dependent nuclear accumulation of zyxin and Akt. *J Clin Invest*. 2005;115:2716–2730.
 29. Chan CB, Liu X, Tang X, Fu H, Ye K. Akt phosphorylation of zyxin mediates its interaction with acinus-S and prevents acinus-triggered chromatin condensation. *Cell Death Differ*. 2007;14:1688–1699.
 30. Xia Y, Sidis Y, Schneyer A. Overexpression of follistatin-like 3 in gonads causes defects in gonadal development and function in transgenic mice. *Mol Endocrinol*. 2004;18:979–994.
 31. Sharpe RM, McKinnell C, Kivlin C, Fisher JS. Proliferation and functional maturation of Sertoli cells, and their relevance to disorders of testis function in adulthood. *Reproduction*. 2003;125:769–784.
 32. Brehm R, Zeiler M, Rüttinger C, et al. A sertoli cell-specific knockout of connexin43 prevents initiation of spermatogenesis. *Am J Pathol*. 2007;171:19–31.
 33. St-Pierre N, Dufresne J, Rooney AA, Cyr DG. Neonatal hypothyroidism alters the localization of gap junctional protein connexin 43 in the testis and messenger RNA levels in the epididymis of the rat. *Biol Reprod*. 2003;68:1232–1240.
 34. Cooke PS, Porcelli J, Hess RA. Induction of increased testis growth and sperm production in adult rats by neonatal administration of the goitrogen propylthiouracil (PTU): the critical period. *Biol Reprod*. 1992;46:146–154.
 35. Cooke PS, Hess RA, Porcelli J, Meisami E. Increased sperm production in adult rats after transient neonatal hypothyroidism. *Endocrinology*. 1991;129:244–248.
 36. Cooke PS, Meisami E. Early hypothyroidism in rats causes increased adult testis and reproductive organ size but does not change testosterone levels. *Endocrinology*. 1991;129:237–243.
 37. Besset V, Le Magueresse-Battistoni B, Collette J, Benahmed M. Tumor necrosis factor alpha stimulates insulin-like growth factor binding protein 3 expression in cultured porcine Sertoli cells. *Endocrinology*. 1996;137:296–303.
 38. Bartholin L, Destaing O, Forissier S, et al. FLRG, a new ADAM12-associated protein, modulates osteoclast differentiation. *Biol Cell*. 2005;97:577–588.
 39. Kato M, Putta S, Wang M, et al. TGF-beta activates Akt kinase through a microRNA-dependent amplifying circuit targeting PTEN. *Nat Cell Biol*. 2009;11:881–889.
 40. Do TV, Kubba LA, Antenos M, Rademaker AW, Sturgis CD, Woodruff TK. The role of activin A and Akt/GSK signaling in ovarian tumor biology. *Endocrinology*. 2008;149:3809–3816.
 41. Bakker CE, Verheij CE, Willemsen R, et al. Fmr1 knockout mice: a model to study fragile X mental retardation. *Cell*. 1994;78:23–33.
 42. Yang B, Song Y, Zhao D, Verkman AS. Phenotype analysis of aquaporin-8 null mice. *Am J Physiol Cell Physiol*. 2005;288:C1161–1170.
 43. Slegtenhorst-Eegdeman KE, de Rooij DG, Verhoef-Post M, et al. Macroorchidism in FMR1 knockout mice is caused by increased Sertoli cell proliferation during testicular development. *Endocrinology*. 1998;139:156–162.
 44. Kooy RF, D'Hooge R, Reyniers E, et al. Transgenic mouse model for the fragile X syndrome. *Am J Med Genet*. 1996;64:241–245.
 45. Shang L, Zhou H, Xia Y, et al. Serum withdrawal up-regulates human SIRT1 gene expression in a p53-dependent manner. *J Cell Mol Med*. 2009;13:4176–4184.
 46. Noriega LG, Feige JN, Canto C, et al. CREB and ChREBP oppositely regulate SIRT1 expression in response to energy availability. *EMBO Rep*. 2011;12:1069–1076.